Supporting Information

Highly Stable Skyrmion State in Helimagnetic MnSi Nanowires

Haifeng Du,[1] John P. DeGrave,[2] Fei Xue,[1] Dong Liang,[2] Wei Ning,[1] Jiyong Yang,[1] Mingliang Tian,[1] Yuheng Zhang [1] and Song Jin [2]**

[1]High Magnetic Field Laboratory, Chinese Academy of Science, Hefei 230031, Anhui, P. R. China; and Hefei National Laboratory for Physical Science at The Microscale, University of Science and Technology of China (USTC), Hefei 230026, People's Republic of China

[2]Department of Chemistry, University of Wisconsin—Madison, 1101 University Avenue, Wisconsin 53706, USA

**Corresponding author: tianml@hmfl.ac.cn and jin@chem.wisc.edu*

I. The parameters of MnSi NW devices investigated in this study

Table 1. The parameters of NW devices for the magnetotransport measurements

Sample numbers	**NW1**	**NW2**	**NW3**
Distance between the voltage electrode (μm)	5.5	3.3	10
Diameter of the wire (nm)	410	390	256
Room temperature resistance (Ω)	81.8	53.4	332.3
Room temperature resistivity ($\mu\Omega.cm$)	240	236	229

II. Fabrication of nanowire devices and technique for transport measurements.

To fabricate NW devices for magnetic transport measurements, a single nanowire grown on the original silicon substrates by CVD method was picked up and transferred onto new clean Si(100) substrates coated with 300 nm silicon oxide by three-axis hanging joystick oil hydraulic micromanipulators under an optical microscope. Four Pt electrodes, as shown in the inset of Fig. 1a, were patterned on an individual wire using focused-ion beam (FIB) technique with a beam current of 7.7 pA using a FEI Helios Nanoab 600i. Prior to the Pt deposition, the contact areas were milled for 5 seconds with a beam current of 7.7 pA in order to remove the surface oxides. The distance between the inner edges of the two voltage electrodes were kept much larger than the spreading distance of Pt or Ga, they are varied from 3μm to 10 μm for three samples used in this work.

Magnetoresistance (MR) measurements were carried out in a physical property measurement system (PPMS, Quantum Design Inc.) by standard 4-probe techniques on individual NWs. Most of our measurements were carried out on three samples, named as NW1 (width ~ 410 nm), NW2 (~ 390 nm) and NW3 (~ 256 nm), respectively. To obtain good

data with high signal-to-noise ratio, a large current of 100 μA and 50 μA were used to measure NW1, NW2 and NW3, respectively. Magnetotransport data under small current were also measured with negligible effects on the experimental results (see Fig. S5 and S6).

III. *Magnetoresistance (MR)* of NW2 above the critical temperature under $H_{\parallel}$

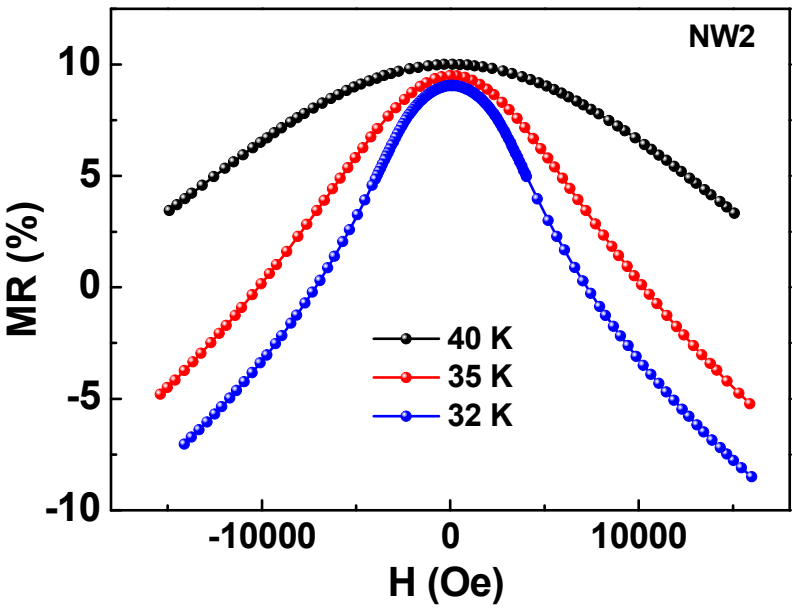

Figure S1. The magnetic field dependence of the *MR* for NW2 above T_c. The negative *MR* data are consistent with the typical results reported in various MnSi materials. The curves are shifted vertically for clarity

IV. Previous reported magnetic phase diagrams for various MnSi morphologies

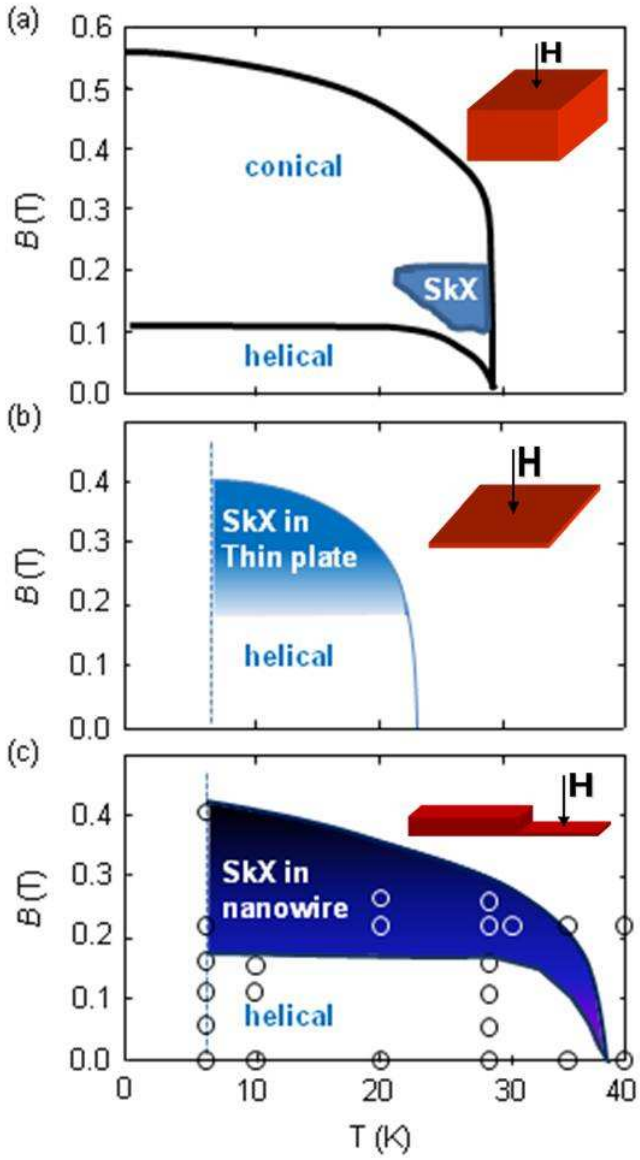

Figure S2. Previous reported magnetic phase diagrams for various MnSi morphologies. (a) Schematic of magnetic phase diagram in bulk MnSi single crystal, (b) mechanically thinned MnSi plate with a thickness of 50 nm, and (c) a FIB-thinned MnSi nanowire with a thickness of 50 nm. The experimental configurations including the samples shape and the orientation of the external magnetic fields *H* are illustrated in the inset. SkX stands for the skyrmion phase. Reprinted from Yu *et al*[1].

V. Magnetotransport data of NW3 under $H_{\parallel}$

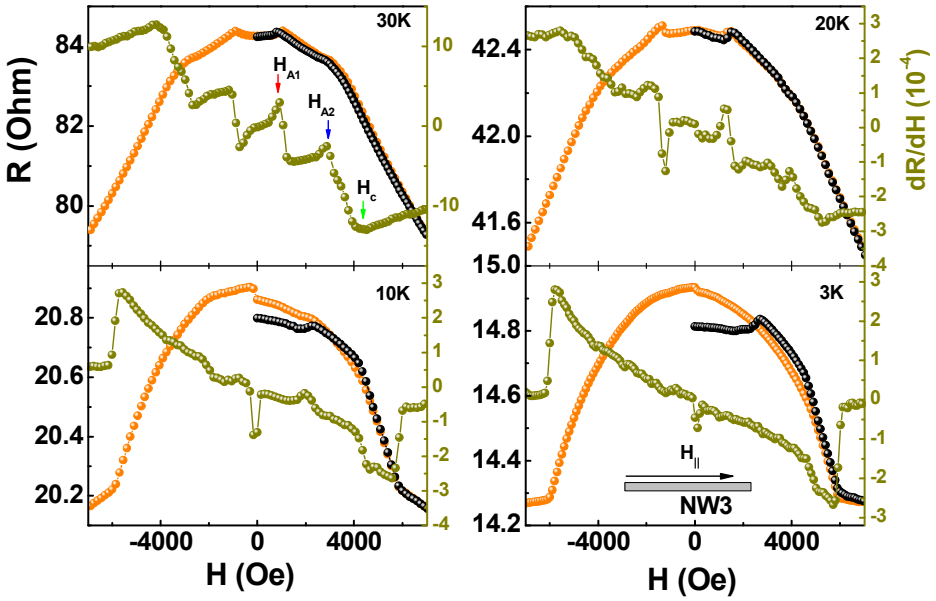

Figure S3. The magnetic field $H_{\parallel}$ dependence of *MR* and its derivative, *dR/dH,* for NW3 at several typical temperatures. The *MR* curves show a distinct change in slope, implying the existence of complex magnetic states including skyrmion states, in agreement with the behaviors of NW1 (see Fig. 2 in the main text).

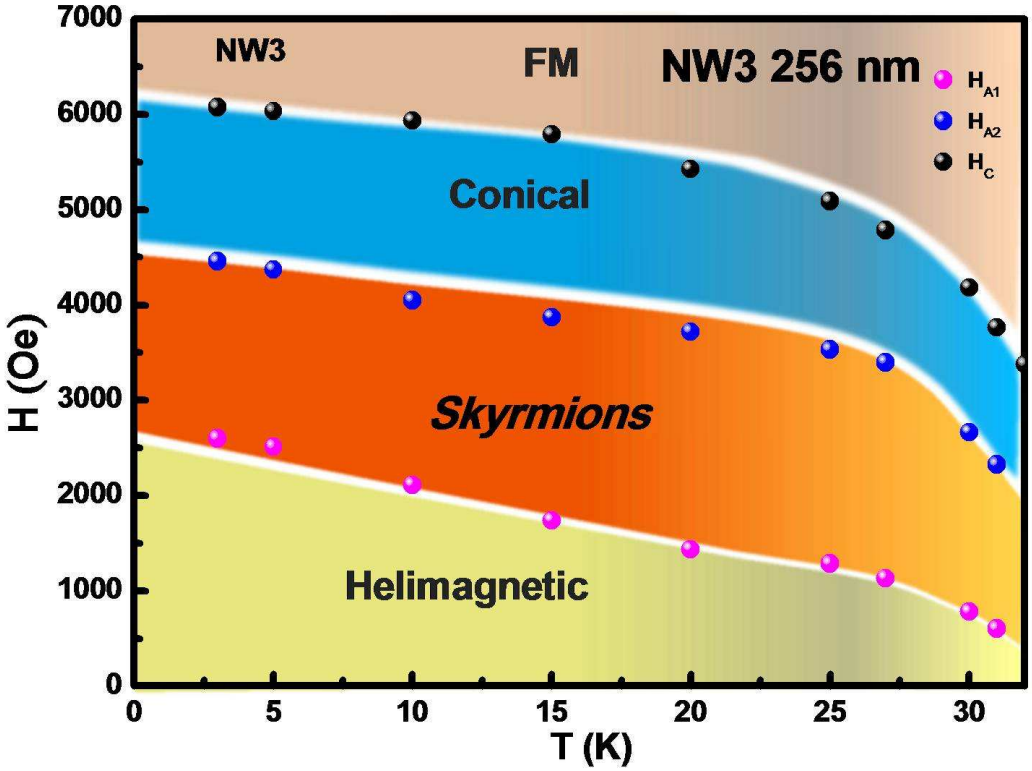

Figure S4. Phase diagram of the MnSi NW inferred from the initial *R(H)* data of NW3. The phase diagram shows close agreement with that of NW1 (see Fig. 4 in the main text) including four different magnetic states. But the critical fields H_{A1} in this sample is slightly higher than that in NW1.

VI. Effect of excitation current on the *MR* data for NW1

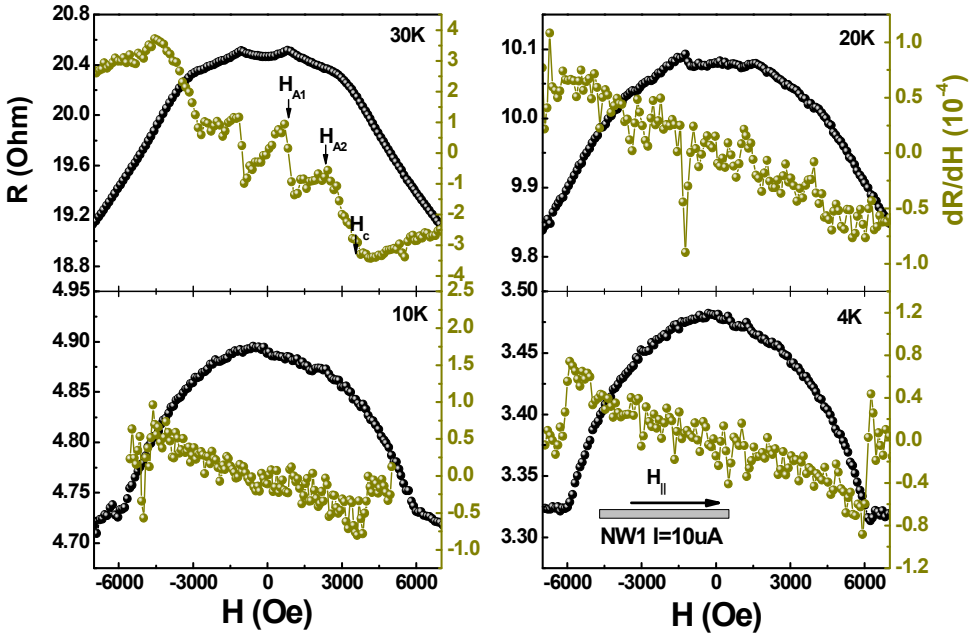

Figure S5. The MR versus $H_{//}$ and its derivative, *dMR/dH,* for NW1 at four typical temperatures measured at an excitation current of 10 μA. The results (see main text Figure 4) show agreement with the case at an excitation current of 100 μA, but give rise to a bad signal-to-noise ratio, especially at low temperature.

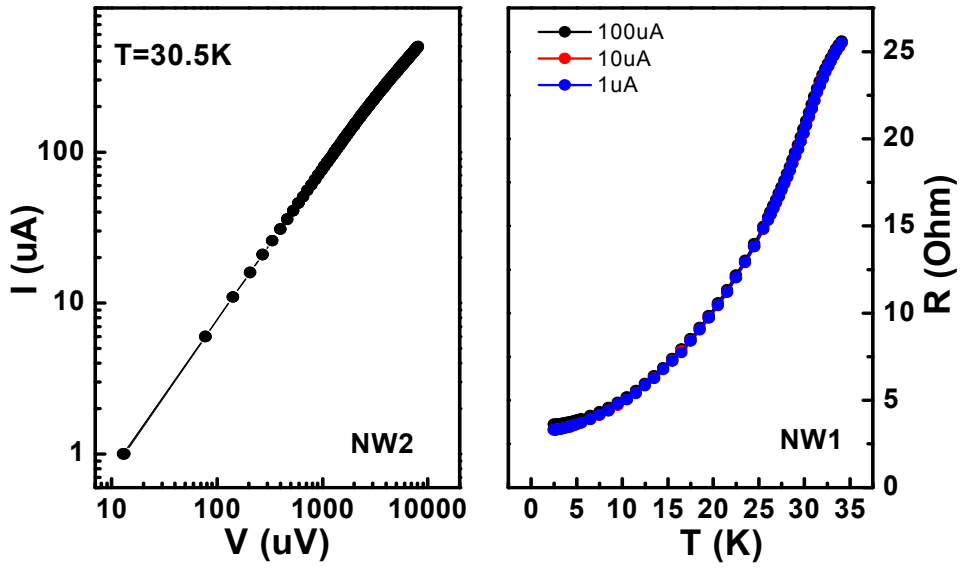

Figure S6. (a) current-voltage (*I-V*) characteristic in double logarithmic scales for a single MnSi NW device for four-probe measurement at *T*=30.5 *K* when I<150 μA. (b) *R(T)* curves recorded at three different currents, 1 μA, 10 μA and 100 μA, respectively. The three curves reproduce nicely, indicating less heating effect at I<100 μA.

Reference:

1. Yu, X. Z.; DeGrave, J. P.; Hara, Y.; Hara, T.; Jin, S.; Tokura. Y. *Nano Lett*. **2013**, 13, 3755–3759. and reference therein.